

The aPKC ζ blocking agent ATM negatively regulates EMT and invasion of hepatocellular carcinoma

CQ Ma¹, Y Yang¹, JM Wang^{*1}, GS Du², Q Shen¹, Y Liu¹, J Zhang¹, JL Hu¹, P Zhu¹, WP Qi¹, YW Qian¹ and Y Fu¹

Epithelial-to-mesenchymal transition (EMT) has an important role in invasion and metastasis of hepatocellular carcinoma (HCC). To explore the regulatory mechanism of atypical protein kinase C ζ (aPKC ζ) signaling pathways to HCC development, and find an agent for targeted therapy for HCC, immortalized murine hepatocytes were employed to establish an EMT cell model of HCC, MMH-RT cells. Our study showed that EMT took place in MMH-R cells under the effect of transforming growth factor- β 1 (TGF- β 1) overexpressing aPKC ζ . Furthermore, we showed that the aPKC ζ blocking agent aurothiomalate (ATM) inhibited EMT and decreased invasion of hepatocytes. Moreover, ATM selectively inhibited proliferation of mesenchymal cells and HepG2 cells and induced apoptosis. However, ATM increased proliferation of epithelial cells and had little effect on apoptosis and invasion of epithelial cells. In conclusion, our result suggested that aPKC ζ could be an important bio-marker of tumor EMT, and used as an indicator of invasion and malignancy. ATM might be a promising agent for targeted treatment of HCC.

Cell Death and Disease (2014) 5, e1129; doi:10.1038/cddis.2014.91; published online 20 March 2014

Subject Category: Cancer

In the last decade, hepatocellular carcinoma (HCC) is considered to be the most lethal of cancers, accounting for approximately one-third of all malignancies.^{1,2} HCC is curable by surgical resection or liver transplantation if diagnosed at early stage.³ However, the risk of 5-year recurrence of HCC following hepatic resection is as high as 50–70%, due to its high invasion and the frequent intra- and/or extra-hepatic metastases.⁴ Epithelial–mesenchymal transition (EMT) has been shown to be a pivotal mechanism contributing to cancer invasion and metastasis, as epithelial cells lose their polarity and acquire the migratory properties of mesenchymal cells. The characteristic changes during EMT include the down-regulation of epithelial markers, such as E-cadherin and the upregulation of mesenchymal markers such as vimentin.⁵ A correlation between the expression profiles of EMT, and tumor recurrence or distant metastasis, has been demonstrated in certain types of cancer, including HCC.^{6–8} Although several EMT-related transcription factors such as Snail, Twist, and Zinc finger E-box binding protein 1 (ZEB1) have been shown to be involved in the process of EMT in HCC,^{9,10} the molecular mechanisms underlying the regulation of EMT in HCC have not yet been fully elucidated.

Atypical protein kinase C ζ (aPKC ζ) is a newly discovered aPKC, which is independent of calcium, diacylglycerol, and is only activated by phospholipids. It is an important signaling molecule taking part in transformation, adhesion, movement, invasion, and metastasis of tumor cells.¹¹ Recent studies

indicated that aPKC ζ is the sole catalytic component of the Par3-Par6-aPKC ζ complex, which has a critical role in the establishment and maintenance of epithelial cell polarity, tight junctions, and adherens junctions.¹² Importantly, loss of apical-basal cell polarity is essential for EMT, a critical step in cellular motility and invasion.¹³ Loss of polarity also allows several growth factors and receptors, which are normally compartmentalized because of tight junctions in polarized cells, to mediate autocrine cell activation.^{14,15}

We previously reported that aPKC ζ expression was higher at both mRNA and protein levels in HCC tissues (44 cases) than in peri-tumoral and normal tissues.¹⁶ Accumulation of aPKC ζ in HCC cytoplasm and nucleolus was found to be associated with the loss of polarity and tight junctions in cell–cell contact and E-cadherin was reduced and accumulation of cytoplasm β -catenin increased in HCC.¹⁶ These observations suggest that overexpression of aPKC ζ may have an important role in the promotion of invasion and metastasis in HCC.¹⁶ Therefore, we are lead to postulate that the aPKC ζ , a key catalytic regulator of polarity and tight junctions, might serve as target for the treatment of HCC.

The current study examined the relation between aPKC ζ signaling pathway and the invasion and metastasis of HCC, with an attempt to identify a new target for the drug therapy of HCC. Immortalized murine hepatocytes (MMH-D3 cell line, obtained from Prof. Marco Tripodi, University La Sapienza, Roma, Italy) were used to establish a cell model of

¹Department of Biliary and Pancreatic Surgery/Cancer Research Center Affiliated Tongji Hospital, Tongji Medical College, Huazhong University of Science and Technology, Wuhan, China and ²Department of General Surgery, Xinqiao Hospital, Third Military Medical University, Chongqing, China

*Corresponding author: JM Wang, Department of Biliary and Pancreatic Surgery/Cancer Research Center Affiliated Tongji Hospital, Tongji Medical College, Huazhong University of Science and Technology, Wuhan 430030, China. Tel/Fax: + 86 027 83665395; E-mail: wjm18jgm@aliyun.com

Keywords: epithelial-to-mesenchymal transition; aPKC ζ ; hepatocellular carcinoma; aurothiomalate; targeted drug

Abbreviations: aPKC ζ , atypical protein kinase C ζ ; ATM, aurothiomalate; CML, chronic myelogenous leukemia; EGF, epidermal growth factor; EMT, epithelial-to-mesenchymal transition; HCC, hepatocellular carcinoma; IGF-II, insulin-like growth factor II; MMH-D3 cells, immortalized murine hepatocytes; MMH-R cells, the MMH-D3 cells were infected with lentiviruses that bicistronically expressed constitutively active v-Ha-Ras and GFP; MMH-RT cells, the MMH-R cells treating with TGF- β 1 signaling; MMP 10, matrix metalloproteinase 10; NSCLC, non-small lung cancer; RA, rheumatoid arthritis; TGF- β 1, transforming growth factor- β 1; ZEB1, zinc finger E-box binding protein 1

Received 11.10.13; revised 08.1.14; accepted 10.2.14; Edited by H-U Simon

hepatocellular tumor invasion and metastasis by treating the cells with oncogenic v-Ha-Ras in combination with transforming growth factor- β 1 (TGF- β 1) signaling. The *in vitro* model was verified by detecting the EMT markers and increased invasion of the cells. Specific blocking agent of aPKC ζ signaling pathway, aurothiomalate (ATM), was used to inhibit the effects of aPKC ζ on invasion, survival, and apoptosis of EMT cells (MMH-RT cells), and then the inhibitory effect was examined to explore the function of aPKC ζ in HCC EMT and to find a target drug for HCC therapy and lay a foundation for further research.

Results

Effect of v-Ha-Ras and TGF- β 1 on aPKC ζ and EMT of hepatocytes. Epithelial MMH-D3 cells were infected with lentiviruses that bicistronically expressed constitutively active v-Ha-Ras and green fluorescent protein (GFP).¹⁷ Flow cytometrically separated GFP-positive cells expressing v-Ha-Ras protein in MMH-D3, MMH-R (24-h post transfection), and MMH-R (passage 1) cells were determined by western blot analysis using the anti-v-Ha-Ras antibody. The result showed that expression of v-Ha-Ras (21 kDa) was significantly higher in MMH-R (24-h post transfection) and MMH-R (passage 1) cells than in MMH-D3 parental cells, as shown in Figure 1a.

To establish a cell model with EMT phenotypes, MMH-R cells were then stimulated with TGF- β 1 for 24 h (MMH-RT cells) and comparable growth rate between MMH-D3, MMH-R, and MMH-RT cells was observed (Figure 1b).¹⁸ In contrast, treatment of these parental MMH-D3 hepatocytes with 8 ng/ml TGF- β 1 resulted in growth inhibition within 72 h. In the following 4 days (4–7 days), this cell growth was consistently inhibited (Figure 1b, Student's *t*-test, $P < 0.05$). The epithelial and mesenchymal markers were examined by western blotting (Figures 1c and d). It was found that the expression of epithelial markers E-cadherin (135 kDa) and β -catenin (92 kDa) was significantly reduced in MMH-RT cells, compared with MMH-R cells (Student's *t*-test, $P < 0.01$). With the loss of epithelial markers, expression of mesenchymal markers such as vimentin (53 kDa) was obviously increased in MMH-RT cells as compared with MMH-R cells (Figures 1c and d, Student's *t*-test, $P < 0.01$). The subcellular distribution of E-cadherin and β -catenin was analyzed under an immunofluorescent microscope. As shown in Figure 1e, E-cadherin and β -catenin were localized at cell–cell junction in MMH-R cells (Figure 1eI, III); however, in MMH-RT cells, E-cadherin was lost from cell boundaries and β -catenin was redistributed diffusely in cytoplasm (Figure 1eII, IV). Consistent with the morphological changes in EMT, MMH-RT cells transformed into spindle shape from triangle form (Figure 1fI–III).

Loss of cell adhesion, disruption of the tight junction, unrestricted proliferation, and increase in mesenchymal markers and morphological changes of MMH-R cells induced by TGF- β 1 all indicated that the phenotype of MMH-RT cells was transformed from epithelia into mesenchymal cells and obtain the unrestricted proliferation ability.

We further detected aPKC ζ (74 kDa) protein and aPKC ζ was also apparently induced by TGF- β 1 in MMH-RT cells, as

was observed with vimentin (Figures 1c and d, Student's *t*-test, $P < 0.01$). Therefore, MMH-RT cells can serve as a suitable model for the study of the invasion and metastasis of HCC regulated by aPKC ζ signaling pathway.

Inhibitory effect of ATM on aPKC ζ and PAR6 binding in PB1 domain. The recombinant plasmids, pET-15b/aPKC ζ and pGEX-4t-3/PAR6, were constructed (Figure 2aI, II) and transformed into *E. coli* (Supplementary Figure 1). The direct binding of PB1 domain of aPKC ζ with PAR6 was verified with GST pull-down assay, and the interaction between aPKC ζ and PAR6 was inhibited by ATM (Figure 2b). The interaction between aPKC ζ and PAR6 was suppressed by ATM in a dose-dependent manner (Figures 2b and c), and the finding was consistent with previously reported results (Alan P Fields). The semiquantitative with western blotting and standardizing IOD showed that the mean binding ratio ($n = 3$) was 63.8% at 10 μ M of ATM and 32.7% at 50 μ M of ATM, respectively, when the ratio was set at 100% at 0 μ M of ATM (Figure 2c). The IC₅₀ of ATM was 20.42 μ M.

To know whether the interaction between aPKC ζ and PAR6 is also inhibited by ATM in MMH-RT cells, we performed co-immunoprecipitation (CO-IP). After 24-h treatment with ATM, an antibody against aPKC ζ was used to immunoprecipitate Par6 protein from cell extracts. The isolated proteins were analyzed by western blotting by using an anti-Par6 antibody. The Par6 bands are shown in Figure 2d, which reveals that protein content dropped gradually with increasing concentration of ATM (the left-hand pictures). On the other hand, a Par6 antibody was used to precipitate aPKC ζ protein and anti-aPKC ζ antibody was employed to detect aPKC ζ . The result exhibited that protein content gradually decreased with increasing concentration of ATM (Figure 2d, the right-hand pictures). The interaction between aPKC ζ and PAR6 was inhibited by ATM in a dose-dependent manner in MMH-RT cells. The mean binding ratios ($n = 3$), as semiquantitatively determined with western blotting, are shown in Figure 2e, with IOD standardized and the ratio at 0 μ M of ATM defined as 100%. The IC₅₀ of ATM was 295.05 μ M with Par6 and 254.57 μ M with aPKC ζ , respectively.

Partial inhibition of transition of epithelial cell markers to mesenchymal cell markers of MMH-RT cells by ATM. To assess the effect of the aPKC ζ signaling pathway on EMT in HCC, we determined EMT markers and aPKC ζ levels in ATM-treated MMH-RT cells (Figure 3a). After 48-h incubation, the expression of aPKC ζ was gradually decreased with increasing concentration of ATM in MMH-RT cells (Figure 3b, Student's *t*-test, $P < 0.05$, $P < 0.01$); the expression of N-cadherin was significantly decreased in MMH-RT cells (Figure 3b, Student's *t*-test, $P < 0.05$); the expression of β -catenin was slightly increased in MMH-RT cells (Figure 3b, Student's *t*-test, $P < 0.05$); the expression of E-cadherin was slightly increased in MMH-RT cells (Figure 3b, Student's *t*-test, $P < 0.05$). Additionally, the expression of vimentin remained unchanged in MMH-RT cells, and bore no association with ATM levels (Figure 3b). These results suggested that the ATM could partially inhibit EMT transition in MMH-RT cells.

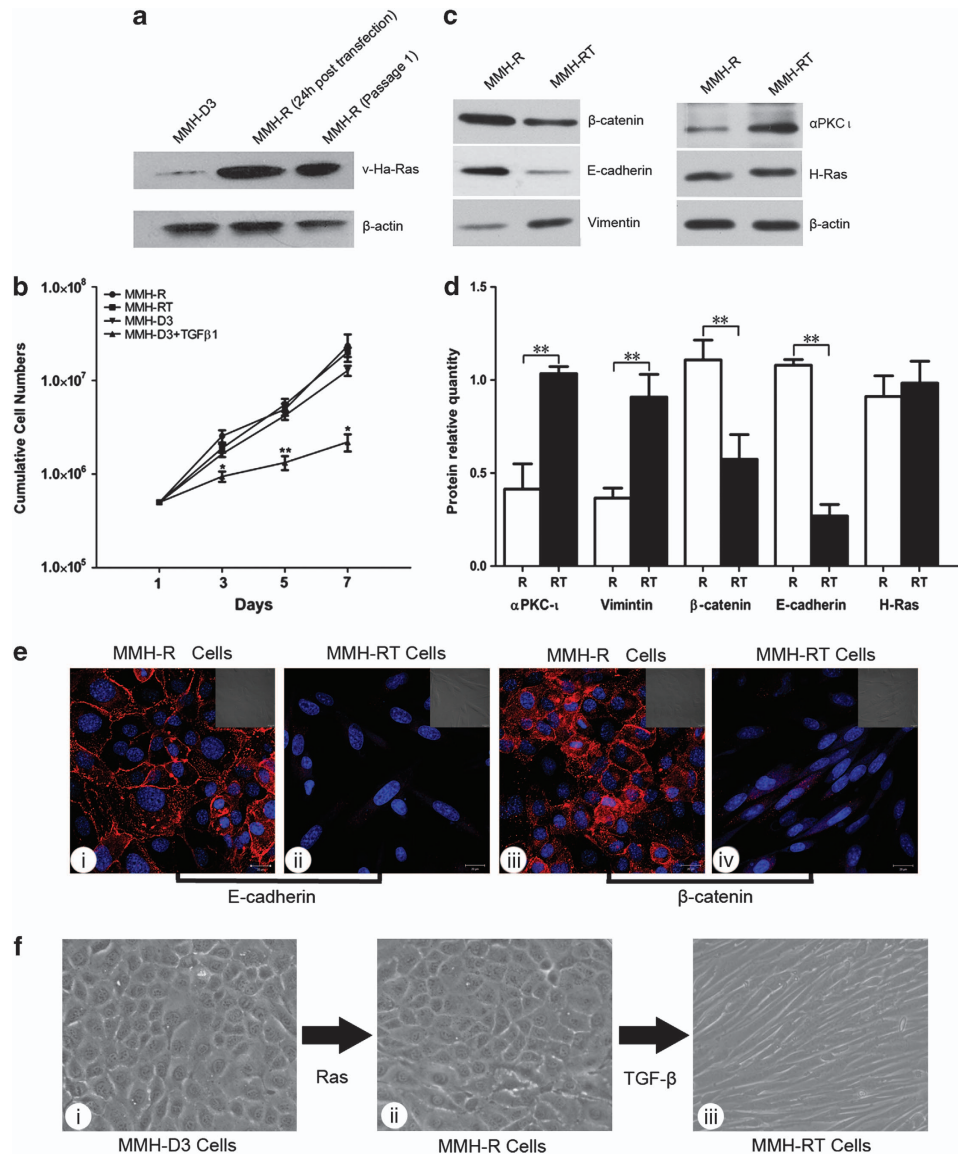


Figure 1 Effect of v-Ha-Ras and TGF- β 1 on aPKC ζ and EMT of hepatocytes. (a) MMH-R cells were infected with oncogenic v-Ha-Ras. The expression levels of v-Ha-Ras were determined by western blot analysis. (b) Proliferation kinetics of MMH-R (circles), MMH-RT (squares), MMH-D3 (inverted triangles) versus MMH-D3 + TGF- β 1 cells (triangles) in 7 days. MMH-RT cells showed proliferation kinetics comparable to the MMH-R and MMH-D3 cells. In contrast, MMH-D3 cells with 8 ng/ml TGF- β 1 resulted in growth inhibition within 72 h ($n=3$, Student's t -test, mean \pm S.D., $*P<0.05$). (c and d) Expression of EMT markers (E-cadherin, β -catenin, and vimentin), v-Ha-Ras, and aPKC ζ in MMH-R and MMH-RT cells was detected by western blot analysis of ($n=3$, Student's t -test, mean \pm S.D., $**P<0.01$). (e) Adherens junction markers E-cadherin and β -catenin were stained with anti-E-cadherin (red), anti- β -catenin (red) and DAPI (blue) by immunocytochemistry. E-cadherin and β -catenin remained restricted to cell-cell boundaries in MMH-R cells (I, III, $\times 200$). But E-cadherin was hardly detected in MMH-RT cells (II, $\times 200$), and β -catenin was diffusely redistributed in cytoplasmic of MMH-RT cells (IV, $\times 200$). (f) No significant differences of morphological changes between MMH-D3 (I, $\times 200$) and MMH-R cells (II, $\times 200$) were observed. Treatment of MMH-R cells (II) with 8 ng/ml TGF- β 1 induced a highly synchronous transition from a polarized, epithelial to a depolarized, spindle-shaped and mesenchymal morphology within 24 h, termed as MMH-RT cells (III, $\times 200$)

Inhibition of viability and invasion of mesenchymal MMH-RT cells by ATM. It was previously shown that ATM was an effective proliferation inhibitor of aPKC ζ signaling in non-small lung cancer (NSCLC) cells.¹⁹ In this study, we focused on the inhibitory effect of aPKC ζ blocking agent ATM on HCC EMT cells. The cell counting kit-8 (CCK8) assay showed that the survival rate of MMH-RT cells decreased rapidly with increasing concentrations and time of ATM treatment (Figures 4a–c). In all, 24, 48, and 72 h after the incubation, the IC₅₀ of MMH-RT cells was 8582.87, 612.98,

and 483.68 μ mol/l, respectively. In contrast, the stimulating effect of ATM on cell proliferation of epithelial MMH-R cells increased with the time of ATM treatment; but the cell proliferation-stimulating effect was not conspicuously correlated with concentration in the concentration range used in this experiment (Figures 4a–c).

The effects of ATM on invasion of MMH-R and MMH-RT cells were evaluated by transwell assay. After induction with TGF- β 1, the invasion was significantly increased in mesenchymal MMH-RT cells than in epithelial MMH-R cells (Figures 4d,

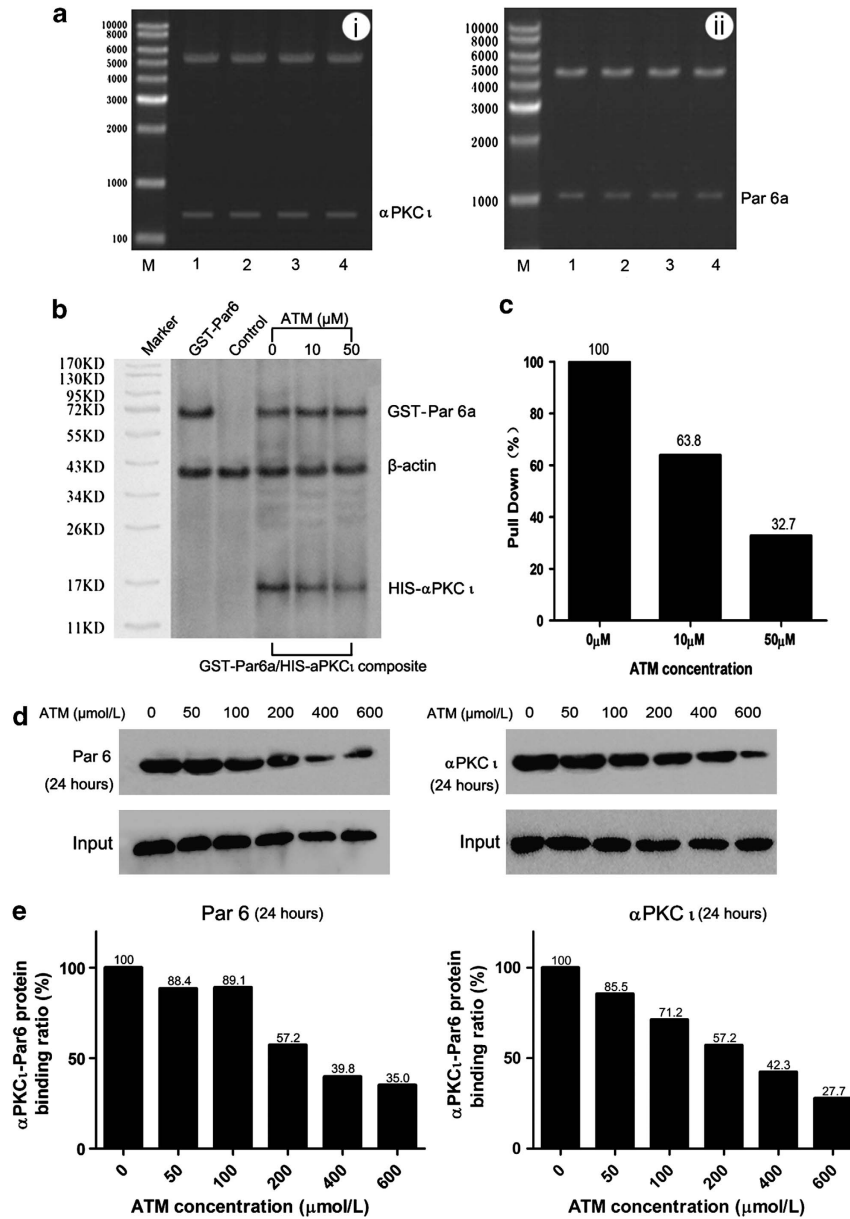


Figure 2 Inhibitory effect of ATM on aPKC ζ and PAR6 binding in PB1 domain. (a) The recombinant plasmids (pET15b/aPKC ζ , pGEX-4T-3/Par6a) were transformed into *E. coli* BL21 (DE3) and the expression of both aPKC ζ and PAR6a was determined with enzyme digestion electrophoresis. M: DNA Maker (DL3000); 1–4 were duplicated samples; (I) aPKC ζ gene was 360 bp; (II) PAR6a gene was 1058 bp. (b) The direct bindings of PB1 domain of aPKC ζ with PAR6 were confirmed and the interaction between aPKC ζ and PAR6 was attenuated with the dosage of ATM. (c) The mean binding ratio of aPKC ζ and PAR6 at 0 $\mu\text{mol/l}$ ATM was defined as 100%, and the ratio was 63.8% at 10 $\mu\text{mol/l}$ ATM and 32.7% at 50 $\mu\text{mol/l}$ ATM as semiquantitatively determined (Gel Pro 4.0 software) by western blotting ($n = 3$). The IC₅₀ of ATM was 20.42 μM . (d) The CO-IP was performed to study the inhibitory effect of ATM on the binding of aPKC ζ with PAR6 in MMH-RT cells. The isolated proteins (aPKC ζ and Par6) were analyzed by western blotting. (e) The mean binding ratio of aPKC ζ and PAR6 at 0 $\mu\text{mol/l}$ ATM was defined as 100% and the ratio was semiquantitatively determined by (Gel Pro 4.0 software) western blotting ($n = 3$). The IC₅₀ of ATM was 295.05 μM with Par6 and 254.57 μM with aPKC ζ , respectively

II and e, Student's *t*-test, $P < 0.01$). The ATM inhibited the invasion of MMH-R cells and MMH-RT cells in a dose-dependent manner in the range of 1–100 $\mu\text{mol/l}$ (Figures 4d and e). However, the sensitivity of MMH-RT cells to ATM was much higher than that of the MMH-R cells. When treated with 10 $\mu\text{mol/l}$ ATM, MMH-R and MMH-RT cells showed similar invasion (Figures 4dIII, IV and e). However, higher concentration of ATM (100 $\mu\text{mol/l}$) significantly decreased the invasion in MMH-RT cells than in MMH-R

cells (Figures 4dV, VI and e, Student's *t*-test, $P < 0.01$). However, no effect of ATM on the morphological change of the cells was observed (Figure 4d). These findings indicated that the aPKC ζ signaling inhibitor could significantly suppress the proliferation and invasion of mesenchymal MMH-RT cells.

Induction of apoptosis of mesenchymal MMH-RT cells by ATM. ATM-induced apoptosis in 48 h was detected by fluorescence activated cell sorter (FACS) (Figure 5a).

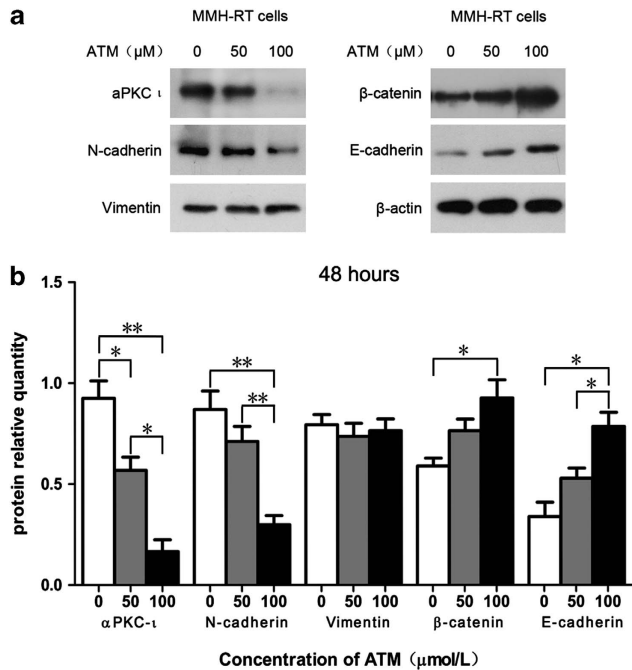


Figure 3 ATM partly inhibited transition from epithelial cell markers to mesenchymal cell markers in MMH-RT cells. (a) Cells were treated with 0, 50, and 100 $\mu\text{mol/l}$ ATM, respectively. After 48 h of incubation, cells were harvested and analyzed by western blotting. (b) Expression of EMT markers (E-cadherin, β -catenin, N-cadherin, and vimentin) and aPKC_i in MMH-RT cells was detected by western blotting ($n=3$, Student's *t*-test, mean \pm S.D., * $P<0.05$, ** $P<0.01$, ImageJ2X software)

The results showed that the standardized apoptotic rate (%) of mesenchymal MMH-RT cells was dramatically higher than that of epithelial MMH-R cells when concentration of ATM treatment was above 200 $\mu\text{mol/l}$ (Figure 5b, Student's *t*-test, $P<0.05$, Supplementary Figure 2), while in MMH-R cells, the apoptosis rate had no obvious correlation with concentration (Figure 5b; Supplementary Figure 2). We also detected the expression of caspase 3, a key molecule of apoptosis signal pathway, in the MMH-R and MMH-RT cells. The results exhibited that the expression of cleaved-caspase 3 of MMH-RT cells was significantly higher than that of MMH-R cells with the increased concentration of ATM (Figure 5c, Student's *t*-test, $P<0.01$). These findings indicated that the aPKC_i signaling inhibitor could activate the caspase 3-dependent apoptosis pathway and significantly promote the apoptosis of MMH-RT cells.

Significant inhibition of viability and promotion of apoptosis of HepG2 cell line with aPKC_i overexpression by ATM. Comparison between MMH-D3 and HepG2 cells revealed that HepG2 cells were hepatocarcinoma cells highly expressing aPKC_i (Figure 6a, Student's *t*-test, $P<0.01$). FACS showed that the apoptotic rate (%) of HepG2 cells was dramatically increased as concentration of ATM was raised up to 50 $\mu\text{mol/l}$ in 48 h (Figures 6b and c, Student's *t*-test, $P<0.05$, $P<0.01$; Supplementary Figure 2). CCK8 assay revealed that HepG2 cells were very sensitive to ATM (Figure 6d). In all, 24, 48, and 72 h after incubation, the IC50 of HepG2 cells was 68.10, 59.93, and 45.59 $\mu\text{mol/l}$, respectively.

The results suggested that ATM had a strong inhibitory effect on hepatocarcinoma cells overexpressing aPKC_i.

Discussion

To examine the role of aPKC_i in invasion and metastasis and outcome of HCC, our previous studies exhibited that the gene and protein expressions of aPKC_i are obviously higher in HCC tissues than in peri-tumor tissues and normal tissues.^{16,20} Accumulation of aPKC_i in HCC cytoplasm and nucleoli was associated with the loss of polarity and tight junctions in cell–cell contact. However, we also found that E-cadherin was reduced and accumulation of cytoplasmic β -catenin was increased in HCC.¹⁶ These studies led us to postulate that the overexpression of aPKC_i may have a critical role in the regulation of EMT in HCC.¹⁶ To explore the roles of aPKC_i signaling pathway in HCC invasion and metastasis and to seek a novel therapeutic target of HCC treatment, we employed the immortalized murine hepatocyte cell line MMH-D3 to establish an EMT cell model MMH-RT,²¹ and our study showed that, under the synergic effect of oncogenic v-Ha-Ras and TGF- β 1, it had loss of cell adhesion, disrupted tight junction, increased mesenchymal markers and related morphological changes.

By using MMH-D3 hepatocytes, we constructed an EMT cell model of HCC.^{18,22} These untransformed murine cells, generated from liver explants of transgenic mice expressing a constitutively active truncated form of the human cyto-Met, stably grow *in vitro* and display characteristics typical of hepatocytes as indicated by morphological, ultrastructural, cytochemical, and functional criteria.^{23,24} In addition, these MMH-D3 cells retain epithelial cell polarity, express hepatocyte-enriched transcription factors and hepatic markers, and maintain their highly differentiated program throughout multiple cell divisions.^{25–27} Furthermore, MMH cells have been previously well characterized as model of TGF β -induced reversible EMT, in which the master regulators Snail and HNF4a have key roles.^{21,28}

Our study showed that TGF- β 1 worked with constitutively active v-Ha-Ras to induce and maintain EMT. This process is accompanied by aPKC_i overexpression. Meanwhile, we also found that ATM could block aPKC_i-Par6 complexes *in vitro* and affect the biological features of MMH-RT. ATM efficiently inhibited transition of epithelial cell markers to mesenchymal cell markers, viability and invasion, but promoted apoptosis of mesenchymal MMH-RT cells. These findings indicated that ATM has more potent inhibitory effect on mesenchymal cells than on epithelial cells. Interestingly, ATM could also significantly inhibit HepG2 cells, a human hepatocarcinoma cell line, which overexpresses aPKC_i. Moreover, our research also showed that ATM could dose-dependently decrease the expression of aPKC_i in mesenchymal MMH-RT cells. These results proved our hypothesis that aPKC_i signaling pathway is essential for efficient TGF- β 1-induced EMT of HCC cells, and inhibition of aPKC_i signaling pathway might be an alternative for the treatment of HCC.

It was previously reported that aPKC_i drives transforming growth and invasion of NSCLC cells through activation of a proliferative aPKC_i-Par6-Rac1-Pak-Mek-Erk signaling axis. It is also found overexpressed and prognostic in multiple types

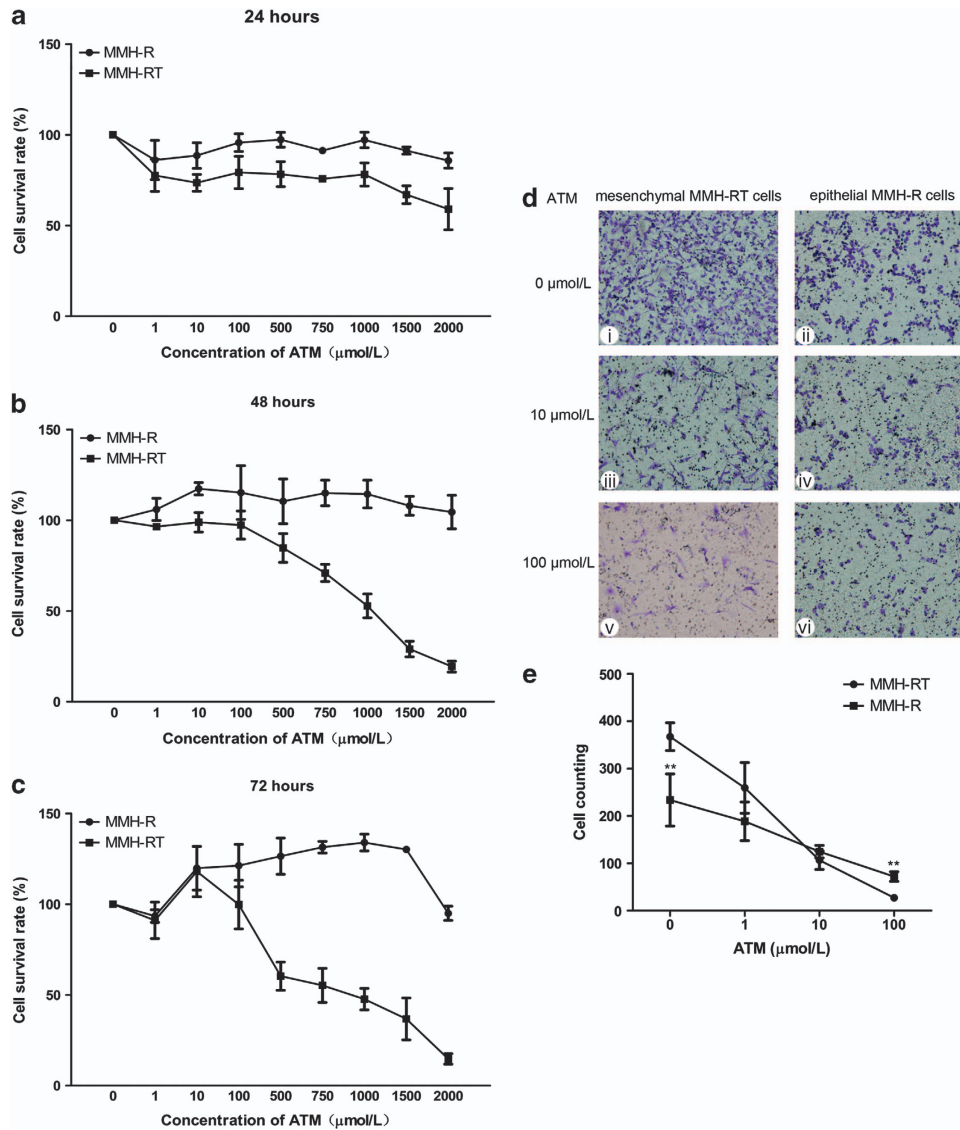


Figure 4 ATM inhibited viability and invasion of mesenchymal MMH-RT cells. (a–c) At 24, 48, and 72 h of incubation with indicated ATM concentration, the survival rates of MMH-R and MMH-RT cells were detected by CCK8 assay ($n=3$, mean \pm S.D.). The ATM demonstrated more potent inhibitory effect on mesenchymal MMH-RT cells (squares) than epithelial MMH-R cells (circles). The IC₅₀ of MMH-RT cells was 8582.87 $\mu\text{mol/l}$ (24 h), 612.98 $\mu\text{mol/l}$ (48 h), and 483.68 $\mu\text{mol/l}$ (72 h), respectively. In contrast, the survival rate of epithelial MMH-R cells increased with prolonged treatment of ATM. (d and e) The invasion of MMH-R and MMH-RT cells was detected by transwell assay ($\times 200$) at 24 h of incubation with indicated ATM concentration ($n=5$, Student's *t*-test, mean \pm S.D., ** $P<0.01$). ATM inhibited the invasion of both MMH-R cells and MMH-RT cells in a dose-dependent manner in a range of 1–100 $\mu\text{mol/l}$, and 100 $\mu\text{mol/l}$ ATM significantly inhibited the invasion of MMH-RT cells than MMH-R cells ($n=5$, Student's *t*-test, mean \pm S.D., ** $P<0.01$)

of cancer.^{29,30} Molecular dissection of signaling downstream of aPKC ζ demonstrated that expression of the PB1 domain of aPKC ζ blocks aPKC ζ -dependent Rac1 activity and inhibits cellular transformation, which indicate a role of this domain in the transforming activity of aPKC ζ .³¹ Recently, Alan P Fields reported that the anti-rheumatoid agent ATM is a potent inhibitor of oncogenic aPKC ζ that blocks the formation of aPKC ζ -Par6 complexes by specifically inhibiting PB1 domain-mediated interactions.^{32–34} In the present work, GST pull down and CO-IP were utilized to examine the blocking effect of ATM on aPKC ζ -Par6 binding. The results showed that the breaking of aPKC ζ -Par6 complex by ATM is dose dependent and with increasing concentrations of ATM, the binding of

aPKC ζ -Par6 was apparently attenuated *in vitro* and in MMH-RT cells.

Until recently, only few studies on the relationship between EMT and aPKC ζ signaling pathway have been performed. Researchers have focused on the effect of aPKC ζ inhibitor on tumor growth, but ignored the regulatory effects of aPKC ζ on epithelial cell adhesion and cell polarization that are involved in tumor EMT, invasion, and metastasis. Recently, it was reported that TGF- β treatment increased endogenous aPKC ζ expression in NSCLC cells and aPKC ζ silencing with siRNA reduced TGF- β -induced EMT.³⁵ This study indicated that TGF- β 1 cooperated with constitutively active v-Ha-Ras to induce and maintain EMT.¹⁸ This process was accompanied

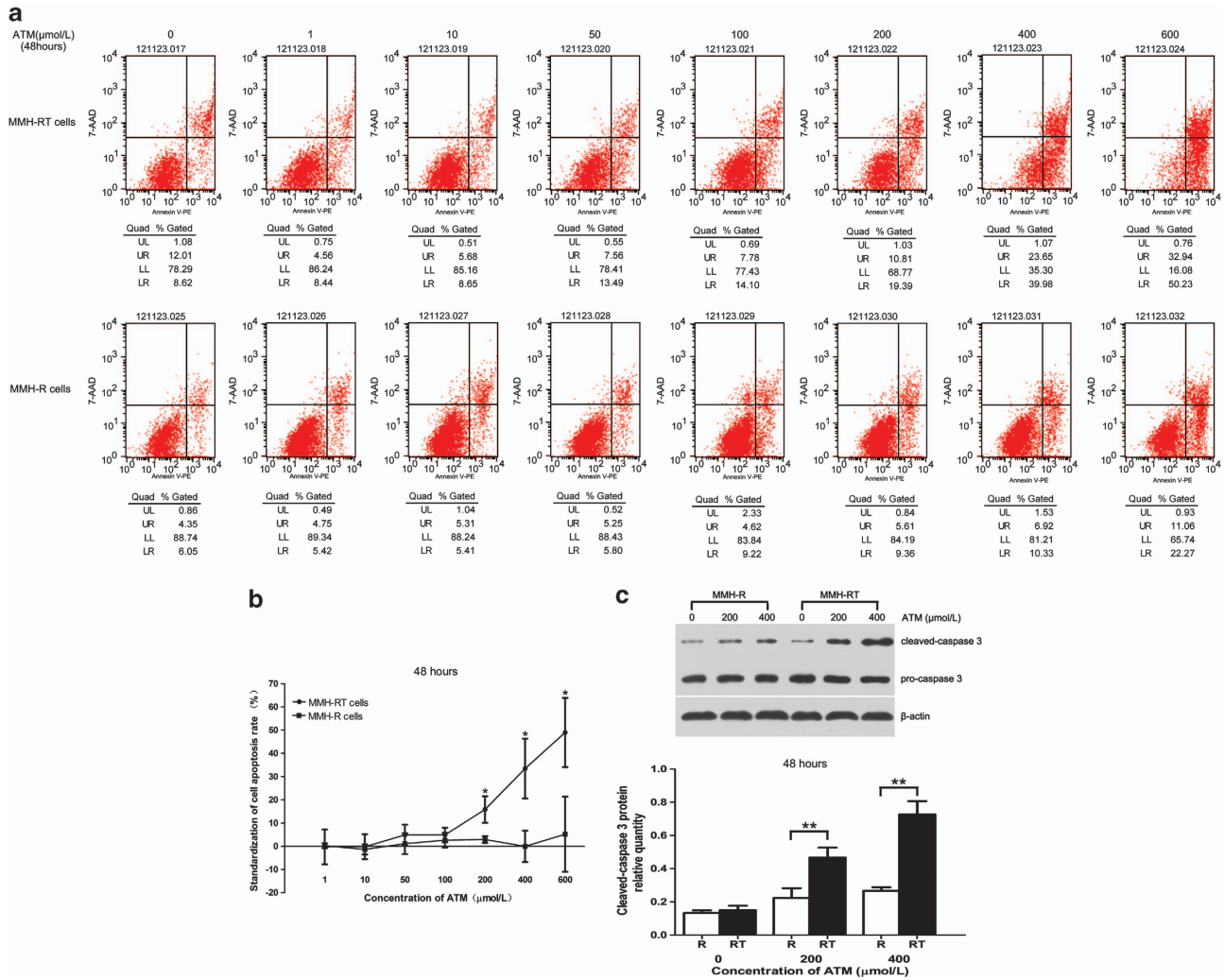


Figure 5 Apoptosis of MMH-R and MMH-RT induced by ATM was determined by flow cytometry. At 48-h ATM incubation in a range of 1–600 $\mu\text{mol/l}$, the apoptotic rates of MMH-R and MMH-RT cells were detected by flow cytometry. (a) Typical FACS schematic. (b) Following the increased ATM concentration, the standardized apoptotic rates (%) of mesenchymal MMH-RT cells were dramatically higher than those of epithelial MMH-R cells when the concentration of ATM treatment was greater than 200 $\mu\text{mol/l}$ ($n=3$, Student's t -test, mean \pm S.D., $*P<0.05$). (c) Expression of caspase 3 (cleaved-caspase 3, pro-caspase 3) in MMH-R and MMH-RT cells was detected by western blotting ($n=3$, Student's t -test, mean \pm S.D., $*P<0.05$, $**P<0.01$, ImageJ2X software)

by loss of cell adhesion, cytoskeletal remodeling, enhanced invasion, and overexpression of aPKC ζ . The results revealed an intimate relationship between the elevated expression of aPKC ζ and the formation and maintenance of EMT. Additionally, ATM not only inhibited the binding between aPKC ζ and Par6 in MMH-RT cells, but also changed their profile of protein expression (from the profile of mesenchymal cells to that of epithelial cells), suppressed the viability and invasion, promoted apoptosis of MMH-RT cells. These findings demonstrated that ATM possesses more potent inhibitory effect on mesenchymal cells than on normal epithelial cells, and aPKC ζ -Par6 signal pathway may cooperate with TGF- β 1 to regulate EMT and cell migration in HCC. We also found that, in mesenchymal MMH-RT cells, the expression of aPKC ζ was gradually decreased with ATM concentration, which was different from the findings by Alan P Fields with carcinoma of lungs. The possible explanation might be that there was a negative feedback regulation loop in the downstream of aPKC ζ signal pathway. When aPKC ζ -Par6 complexes were

decreased, increased free aPKC ζ and blocked downstream signal transduction would lead to a downregulated expression of aPKC ζ by reactively regulating the translation and the expression.

Although present researches provide a compelling rationale for applying ATM for the clinical treatment of HCC, but the precise mechanism by which ATM inhibits tumors is still unknown. In a study of lung cancer, ATM was used as a highly sensitive PB1-PB1 blocker to inhibit the binding between aPKC ζ and Par6, and was found to uncouple aPKC ζ from the downstream Par6-Rac1 effector pathways.^{19,36–38} These results provide a plausible unifying molecular mechanism that could account for both the inhibited proliferation and invasion of ATM. The aPKC ζ -Par6 complex functions to activate a Rac1-Mek-Erk signaling axis that drives the transformed growth of NSCLC cells and then activates downstream signaling molecules matrix metalloproteinase 10 (MMP 10), which has an important role in promoting cell invasion.^{39,40} We also found that ATM is a specific inhibitor of PB1 domain-mediated interaction,

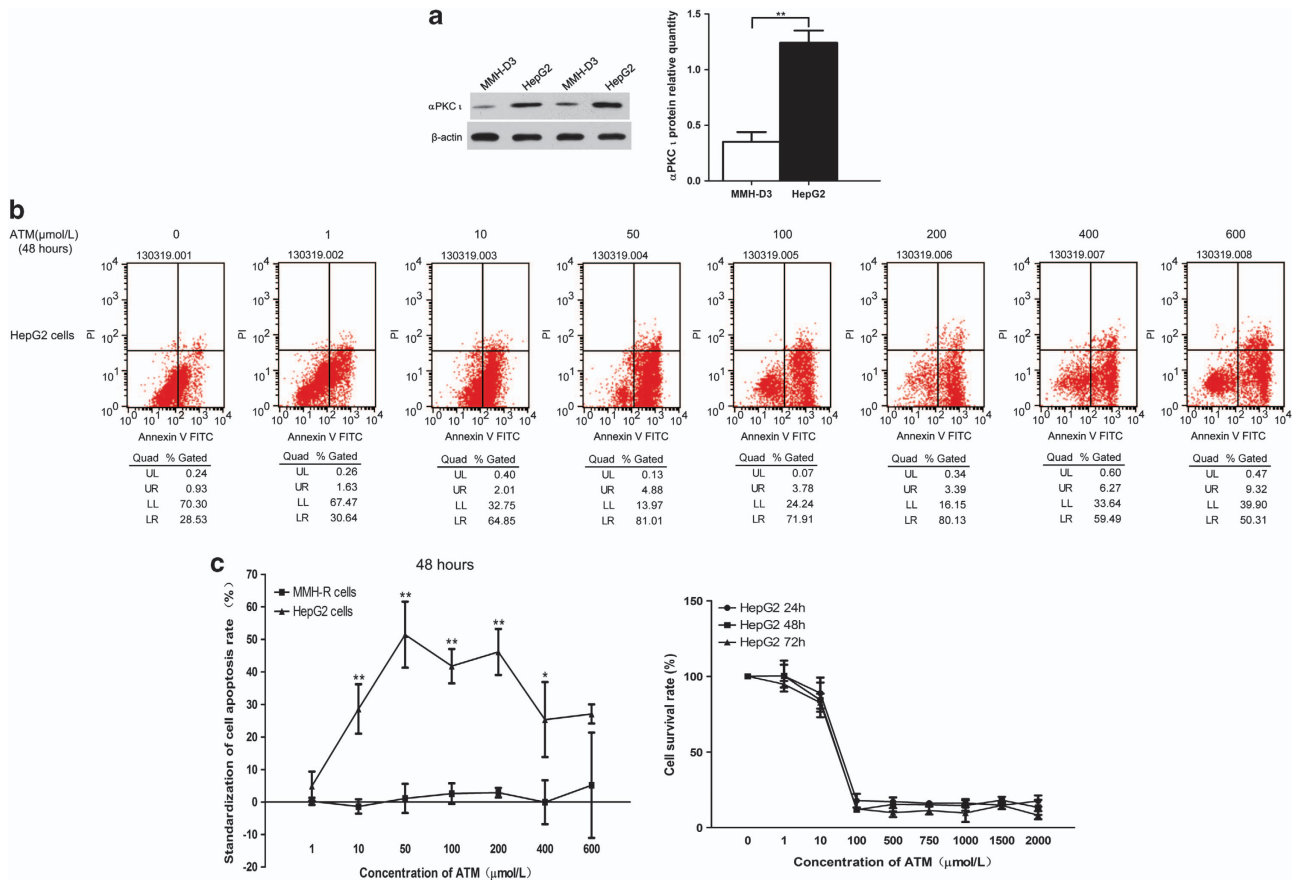


Figure 6 ATM significantly inhibited viability of hepatocarcinoma cell line HepG2 and promoted apoptosis of HepG2 cells which has abundant aPKC ζ expression. (a) The difference of aPKC ζ expression in HepG2 and MMH-D3 cells was detected by western blotting ($n = 3$, Student's t -test, mean \pm S.D., $**P < 0.01$). (b) At 48-h ATM incubation in a range of 1–600 $\mu\text{mol/L}$, the apoptotic rates of HepG2 cells were detected by flow cytometry. (c) Following the raised ATM concentration, the standardized apoptotic rates (%) of both HepG2 and MMH-R cells were detected by flow cytometry ($n = 3$, Student's t -test, Mean \pm S.D., $*P < 0.05$, $**P < 0.01$). (d) At 24 h (circles), 48 h (squares), 72 h (triangles) of ATM incubation with indicated concentration, the survival rates of HepG2 cells were detected by CCK8 assay ($n = 3$, mean \pm S.D.), and the IC50 was 68.10, 59.93, and 45.59 $\mu\text{mol/L}$, respectively

and could block aPKC ζ -mediated activation of Rac1 in MMH-RT cells. So, we postulate that ATM might have an inhibitory effect on MMP 10 in hepatoma cells. But the exact mechanism warrants further study.

Previous study demonstrated that the antitumorigenic effects of ATM are mediated through direct inhibition aPKC ζ -Par6-Rac1 pathway of tumor cell proliferation, instead of tumor cell apoptosis or tumor vascularization in NSCLC.¹⁹ Another study showed that ATM induced apoptotic effects through inhibiting not only the aPKC ζ -Par6-Rac1 pathway but also the aPKC ζ -p62-NF- κ B pathway in chronic myelogenous leukemia (CML) cells.^{30,41} However, a recent research revealed that ATM sensitivity is positively correlated with expression of aPKC ζ and Par6, but not with that of the aPKC ζ -binding protein p62, or thioredoxin reductase 1 or 2, the proposed targets of ATM in rheumatoid arthritis (RA).¹⁹ In our study, low concentration ATM remarkably inhibited the expression of aPKC ζ dose-dependently in MMH-RT cells. ATM also could remarkably induce the expression of cleaved-caspase 3 and promote the apoptosis of MMH-RT cells in a dose-dependent manner. On the basis of the previous findings with CML, we were led to postulate that when ATM inhibited the expression of aPKC ζ , it also indirectly

decreased the signal transduction efficiency of NF- κ B pathway and eliminated the inhibition of apoptosis pathway. The cleaved-caspase 3 was activated and the apoptosis was enhanced. However, involvement of aPKC ζ -p62-NF- κ B pathway in aPKC ζ -mediated resistance to apoptosis in HCC still needs further investigation.

In summary, the above results exhibited that aPKC ζ has a pivotal role in EMT. Taken together, our previous findings with HCC tissues and results with EMT cell models in this study, suggested that signal pathway induced by aPKC ζ works with EMT induced by TGF- β 1 and Ras interaction, promote invasion and metastasis of carcinoma and resist apoptosis together. aPKC ζ could be regarded as one of the critical bio-markers of HCC EMT, and could be used as an indicator of tumor invasion and malignancy. This research also indicated that ATM exerted, via aPKC ζ signal pathway, powerful and versatile antitumor effects and could regulate EMT process. Although the exact underlying mechanisms remain unclear, the proliferation, apoptosis, and invasion of MMH-RT and HCC cells could be regulated by both blockade of aPKC ζ signal pathway and the secondary decrease in aPKC ζ . These results suggested that ATM has potential to be used for the target therapy of HCC.

Materials and Methods

Cell culture and lentivirus transfection. Immortalized Met murine hepatocytes (MMH-D3) were cultured in RPMI-1640 (Hyclone, Logan, UT, USA) supplemented with 10% fetal bovine serum (FBS; Gibco, Grand Island, NY, USA), 50 ng/ml recombinant human epidermal growth factor (EGF; Peprotech, Rocky Hill, CT, USA), 30 ng/ml recombinant human insulin-like growth factor II (IGF-II; Sigma, St. Louis, MO, USA), 10 μ g/ml insulin (Sigma) and 100 U/ml antibiotics.

MMH-R cells were established by transfecting lentivirus (PLL3.7 lentivirus vector; Shanghai Gene Chem Co., Ltd, Shanghai, China) to parental MMH-D3 cells with a vector bicistronically expressing constitutive active v-Ha-Ras (amino acids 177–690, GenBank NO: BC006499.2) and GFP.¹⁷ Selection and propagation of a v-Ha-Ras/GFP-positive cell population were performed by subculturing at a ratio of 1 : 3 twice a week in medium containing growth factors as described for MMH-D3 cells.

Mesenchymal-converted MMH-RT cells were cultured in RPMI-1640 supplemented with 10% FBS, 6–8 ng/ml recombinant human TGF- β 1 (Peprotech) and antibiotics. HepG2 cells (obtained from China Center for Type Culture Collection, Wuhan, China) were cultured in DMEM (Hyclone) supplemented with 10% FBS and 100 U/ml antibiotics. All cells were kept at 37°C in 5% CO₂ and routinely screened for the absence of mycoplasma. ATM (Merck, Darmstadt, Germany) was dissolved by purified water and sterile filtration. The different concentrations of ATM were added to the medium when necessary. Images were captured by using Olympus BX-41 (Olympus, Tokyo, Japan).

Western blot assay. Cells were washed once with ice-cold phosphate-buffered saline (PBS) and lysed with 0.1–0.2 ml RIPA lysis buffer. The protein concentration was determined by Coomassie protein assay (Pierce, Rockford, IL, USA). Proteins were separated by SDS-polyacrylamide gel electrophoresis (SDS-PAGE; Bio-Rad, Hercules, CA, USA), and transferred onto a nitrocellulose membrane (Amersham, Chalfont, UK). The membranes were incubated with primary antibodies (aPKC ζ , Santa Cruz Biotechnology, Santa Cruz, CA, USA; E-cadherin, Cell Signaling Technology, Danvers, MA, USA; Par6, Santa Cruz Biotechnology; β -catenin, Cell Signaling Technology; Vimentin, Cell Signaling Technology; N-cadherin, R&D Systems, Minneapolis, MN, USA; v-Ha-Ras, Santa Cruz Biotechnology; Caspase 3, Santa Cruz Biotechnology) at 4°C overnight. Peroxidase-conjugated secondary antibodies were applied for 60 min at room temperature at a dilution of 1 : 2000. β -Actin (Santa Cruz Biotechnology) was used as the internal control. Peroxidase activity was detected by using chemiluminescence method (Amersham) and visualized on X-Omat S films (Amersham). To quantify the relative levels of protein expression, the intensity of the specific bands was estimated by the ImageJ2X analysis software package (National Institute of Mental Health, Bethesda, MD, USA).

Proliferation assay. In all, 5×10^5 cells were cultured in quintuplicate on petri dishes (10 cm in diameter) with medium containing growth factors indicated above. The cells were counted by detaching with trypsin solution and survival cells were counted under a light microscope after trypan blue staining. The assays were repeated at least three times.

Immunofluorescence assay. MMH-R and MMH-RT cells were seeded onto coverslips, incubated overnight and then fixed with 4% paraformaldehyde. Cells were incubated with primary antibodies (E-cadherin, 1 : 100, Santa Cruz Biotechnology; β -catenin, 1 : 100, Santa Cruz Biotechnology) for 1 h at room temperature. Cy3-dye-conjugated secondary antibodies (Jackson Laboratories, West Grove, PA, USA) were added for 30 min at room temperature at a dilution of 1 : 150 in PBS. Cells were then mounted with Mounting Medium containing DAPI (Vector Laboratories, Burlingame, CA, USA). Images were captured by utilizing a Carl Zeiss LSM 710 laser scanning confocal microscope (Carl Zeiss, Oberkochen, Germany).

Plasmid cloning and expression of recombinant proteins. The PB1 domain of human aPKC ζ (amino acids 1–113, GenBank NO: 5584) and Par6a (cgs, GenBank NO: 50855) was chemically synthesized and separately cloned to prokaryotic expression vectors pET-15b (Novagen, Merck, Germany) and pGEX4T-3 (Amersham Biosciences, GE Healthcare Bio-Sciences, Inc., Pittsburgh, PA, USA) to construct pET-15b/aPKC ζ and pGEX-4t-3/Par6. Genes were sequenced by Invitrogen Co. (Shanghai, China). The recombinant plasmids pET15b/aPKC ζ and pGEX-4T-3/Par6a were transformed into *E. coli* strain BL21 (DE3). Expression of recombinant protein HIS-aPKC ζ and GST-PAR6 was induced with IPTG and determined with SDS-PAGE.

GST pull-down assay. Recombinant HIS-aPKC ζ and GST-PAR6 were used as a bait protein to perform GST pull down. For each GST pull-down experiment, 800 μ l cell lysate from cells treated with ATM (0, 10, and 50 μ M) was added into Handeepin column fixed with GST-PAR6 bait protein and incubated for at least 1 h at 4°C. The column was washed five times with 400 μ l ProFound lysis buffer, incubated for 5 min after mixing in 250 μ l glutathione solution (31 mg/ml) and centrifuged at 1250 \times g for 30 s to 1 min in a collection tube. Eluent was collected and dissolved in a 10% SDS-PAGE gel. The gel was stained with Coomassie blue or applied to immunoblot (rabbit GST antibody, 1 : 200, ProMab Biotechnologies, Inc., Richmond, CA, USA; rabbit HIS antibody, 1 : 200, ProMab Biotechnologies, Inc.; rabbit β -actin antibody, 1 : 200, ProMab Biotechnologies, Inc.). The intensity of the specific bands was estimated by employing Gel pro 4.0 software package (Media Cybernetics, Inc., Rockville, MD, USA). The assays were repeated at least three times.

CO-IP assay. MMH-RT cells were cultured with ATM (0, 10, 50, 100, 200, and 400 μ M). After 24 h, cells were washed once with ice-cold PBS and lysed in RIPA lysis buffer with 1 mM PMSF. The protein concentration was determined by Coomassie protein assay (Pierce). In 200 μ g of cell proteins, rabbit antibody IgG (1 μ g) was dropwise added with protein A/G plus-agarose beads (Beyotime Institute of Biotechnology, Haimen, China) 20 μ l, and rotated for 2 h at 4°C to get rid of non-specific combination. The mixture was centrifuged and the supernatant was collected. CO-IP was performed using rabbit anti-aPKC ζ monoclonal antibody (1 μ g) or mouse anti-Par6 monoclonal antibody (1 μ g) to bind Par6 protein or aPKC ζ protein, respectively. The protein-antibody immunoprecipitates were collected by protein A/G plus-agarose beads. The samples were washed with RIPA buffer five times. Following the final wash, the beads were resuspended in 20 μ l of SDS loading buffer. Finally, the samples were boiled and centrifuged to pellet the agarose beads. The supernatant was collected for western blot detection using the Par6 antibody (1 : 1000) or aPKC ζ antibody (1 : 500) and proper second antibody. The intensity of the specific bands was estimated by Image J2X software package. The assays were repeated at least three times.

Viability assay. Cell viability was colorimetrically assessed using the CCK8 (1 : 10, Dojindo Laboratories Co., Ltd, Kumamoto, Japan). Cells were seeded into 96-well plates at a density of 5×10^3 cells/well in 200 μ l culture medium. In all, 24, 48, and 72 h after the culture, the medium was removed by aspiration and replaced with 100 μ l of experimental medium. In all, 10 μ l CCK8 solution was added to each well and the plates were incubated for 1–4 h at 37°C. Absorbance was recorded at 450 nm using the μ Quant ELISA Reader (Bio Tek Instruments, Inc., Winooski, VT, USA). The percentage of survival rate was calculated according to the following formula: survival rate % = $(OD_{\text{treated}} - OD_{\text{blank}}) / (OD_{\text{control}} - OD_{\text{blank}}) \times 100\%$. IC50 was calculated using probit regression analysis. The assays were conducted in triplicate and repeated at least three times.

Cell invasion. Cells invasion was detected using transwell assay (8 μ m pore size; Corning Costar Corp, Corning Incorporated, Corning, NY, USA). The transwell inserts were put into the 24-well plates and coated with Matrigel (BD Biosciences, Franklin Lakes, NJ, USA). Freshly trypsinized and washed cells were suspended in 200 μ l of RPMI-1640 containing 1% FBS. In all, 1×10^4 cells/well were placed in the top chamber of each insert and 600 μ l of RPMI-1640 containing 10% FBS was added into the lower chambers. After incubation for 24 h at 37°C in a 5% CO₂ humidified incubator, cells were fixed with 95% absolute alcohol and stained with crystal violet. The cells in the inner chamber were removed with a cotton swab and cells attached to the bottom side of the membrane were counted and imaged under an Olympus BX-41 microscope (Olympus) at \times 200 magnification over four random fields in each well. Each experiment was performed in triplicate.

Flow cytometry. Cells were seeded onto 12-well plates at a cell density of 1×10^5 cells/well in 1.5 ml of culture medium and allowed to adhere overnight. Twenty-four hours after the culture, the medium was removed by aspiration and replaced with 1.5 ml of experimental medium containing 0, 1, 10, 100, 200, 400, and 600 μ M ATM. Forty-eight hours after the incubation, the cells were harvested and apoptosis was flow cytometrically determined by using Annexin V-PE/7-AAD and Annexin V-FITC/PI apoptosis detection kit (KeyGen Biotechnology Co., Ltd, Nanjing, China) according to the manufacturer's instructions. The standardization of apoptosis rate was calculated according to the following formula: standardized apoptosis rate (%) = apoptosis rate (%)_{treated} - apoptosis rate (%)_{control}. All experiments were conducted at least three times with similar results.

Statistical analysis. Data were statistically analyzed by using the software package SPSS (version 19.0) for Windows supplied by the Statistics Teaching Room of Tongji Medical College, Huazhong University of Science and Technology. Statistical significance was assessed by means of Student's *t*-test. Results were presented as mean \pm standard deviation (S.D.) unless otherwise stated and difference was considered to be significant when * $P < 0.05$ and ** $P < 0.01$.

Conflict of Interest

The authors declare no conflict of interest.

Acknowledgements. We were indebted to Professor Marco Tripodi (Universita La Sapienza, Italy) who provided MMH-D3 cells and valuable suggestions in the preparation of the manuscript. This work was supported by National Natural Science Foundation of China (grant numbers 30672040, 81072000, and 81172015 to Professor Jianming Wang).

- Montalto G, Cervello M, Giannitrapani L, Dantona F, Terranova A, Castagnetta LA. Epidemiology, risk factors, and natural history of hepatocellular carcinoma. *Ann NY Acad Sci* 2002; **963**: 13–20.
- Llovet JM, Burroughs A, Bruix J. Hepatocellular carcinoma. *Lancet* 2003; **362**: 1907–1917.
- Finn RS. Development of molecularly targeted therapies in hepatocellular carcinoma: where do we go now? *Clin Cancer Res* 2010; **16**: 390–397.
- Mima K, Hayashi H, Kuroki H, Nakagawa S, Okabe H, Chikamoto A et al. Epithelial-mesenchymal transition expression profiles as a prognostic factor for disease-free survival in hepatocellular carcinoma: clinical significance of transforming growth factor-beta signaling. *Oncol Lett* 2013; **5**: 149–154.
- Thiery JP, Aclouque H, Huang RY, Nieto MA. Epithelial-mesenchymal transitions in development and disease. *Cell* 2009; **139**: 871–890.
- Moody SE, Perez D, Pan TC, Sarkisian CJ, Portocarrero CP, Sterner CJ et al. The transcriptional repressor Snail promotes mammary tumor recurrence. *Cancer Cell* 2005; **8**: 197–209.
- Shiomi M, Shida T, Koda K, Oda K, Seike K, Nishimura M et al. Slug expression is an independent prognostic parameter for poor survival in colorectal carcinoma patients. *Br J Cancer* 2006; **94**: 1816–1822.
- van Zijl F, Zulehner G, Petz M, Schneller D, Kornauth C, Hau M et al. Epithelial-mesenchymal transition in hepatocellular carcinoma. *Future Oncol* 2009; **5**: 1169–1179.
- Yang MH, Chen CL, Chau GY, Chiou SH, Su CW, Chou TY et al. Comprehensive analysis of the independent effect of twist and snail in promoting metastasis of hepatocellular carcinoma. *Hepatology* 2009; **50**: 1464–1474.
- Zhou YM, Cao L, Li B, Zhang RX, Sui CJ, Yin ZF et al. Clinicopathological significance of ZEB1 protein in patients with hepatocellular carcinoma. *Ann Surg Oncol* 2012; **19**: 1700–1706.
- Suzuki A, Akimoto K, Ohno S. Protein kinase C lambda/iota (PKClambda/iota): a PKC isotype essential for the development of multicellular organisms. *J Biochem* 2003; **133**: 9–16.
- Macara IG. Parsing the polarity code. *Nat Rev Mol Cell Biol* 2004; **5**: 220–231.
- Thiery JP. Epithelial-mesenchymal transitions in tumour progression. *Nat Rev Cancer* 2002; **2**: 442–454.
- Balci MS, Garrett MD, Matter K. The ZO-1-associated Y-box factor ZONAB regulates epithelial cell proliferation and cell density. *J Cell Biol* 2003; **160**: 423–432.
- Vermeer PD, Einwalter LA, Moninger TO, Rokhlina T, Kern JA, Zabner J et al. Segregation of receptor and ligand regulates activation of epithelial growth factor receptor. *Nature* 2003; **422**: 322–326.
- Du GS, Wang JM, Lu JX, Li Q, Ma CQ, Du JT et al. Expression of P-aPKC-iota, E-cadherin, and beta-catenin related to invasion and metastasis in hepatocellular carcinoma. *Ann Surg Oncol* 2009; **16**: 1578–1586.
- Redmond SM, Reichmann E, Muller RG, Friis RR, Groner B, Hynes NE. The transformation of primary and established mouse mammary epithelial cells by p21-ras is concentration dependent. *Oncogene* 1988; **2**: 259–265.
- Gotzmann J, Huber H, Thallinger C, Wolschek M, Jansen B, Schulte-Hermann R et al. Hepatocytes convert to a fibroblastoid phenotype through the cooperation of TGF-beta1 and Ha-Ras: steps towards invasiveness. *J Cell Sci* 2002; **115**(Pt 6): 1189–1202.
- Regala RP, Thompson EA, Fields AP. Atypical protein kinase C iota expression and aurothiomalate sensitivity in human lung cancer cells. *Cancer Res* 2008; **68**: 5888–5895.
- Wang JM, Li Q, Du GS, Lu JX, Zou SQ. Significance and expression of atypical protein kinase C-iota in human hepatocellular carcinoma. *J Surg Res* 2009; **154**: 143–149.
- Santangelo L, Marchetti A, Cicchini C, Conigliaro A, Conti B, Mancone C et al. The stable repression of mesenchymal program is required for hepatocyte identity: a novel role for hepatocyte nuclear factor 4alpha. *Hepatology* 2011; **53**: 2063–2074.
- Gotzmann J, Fischer AN, Zojer M, Mikula M, Proell V, Huber H et al. A crucial function of PDGF in TGF-beta-mediated cancer progression of hepatocytes. *Oncogene* 2006; **25**: 3170–3185.
- Amicone L, Galimi MA, Spagnoli FM, Tommasini C, De Luca V, Tripodi M. Temporal and tissue-specific expression of the MET ORF driven by the complete transcriptional unit of human A1AT gene in transgenic mice. *Gene* 1995; **162**: 323–328.
- Bellovino D, Lanyau Y, Garaguso I, Amicone L, Cavallari C, Tripodi M et al. MMH cells: An *in vitro* model for the study of retinol-binding protein secretion regulated by retinol. *J Cell Physiol* 1999; **181**: 24–32.
- Amicone L, Spagnoli FM, Spath G, Giordano S, Tommasini C, Bernardini S et al. Transgenic expression in the liver of truncated Met blocks apoptosis and permits immortalization of hepatocytes. *EMBO J* 1997; **16**: 495–503.
- Aiuti A, Cicchini C, Bernardini S, Fedele G, Amicone L, Fantoni A et al. Hematopoietic support and cytokine expression of murine-stable hepatocyte cell lines (MMH). *Hepatology* 1998; **28**: 1645–1654.
- Spagnoli FM, Amicone L, Tripodi M, Weiss MC. Identification of a bipotential precursor cell in hepatic cell lines derived from transgenic mice expressing cyto-Met in the liver. *J Cell Biol* 1998; **143**: 1101–1112.
- Cicchini C, Filippini D, Coen S, Marchetti A, Cavallari C, Laudadio I et al. Snail controls differentiation of hepatocytes by repressing HNF4alpha expression. *J Cell Physiol* 2006; **209**: 230–238.
- Murray NR, Kalari KR, Fields AP. Protein kinase Ciota expression and oncogenic signaling mechanisms in cancer. *J Cell Physiol* 2011; **226**: 879–887.
- Erdogan E, Lamark T, Stallings-Mann M, Lee J, Pellecchia M, Thompson EA et al. Aurothiomalate inhibits transformed growth by targeting the PB1 domain of protein kinase C iota. *J Biol Chem* 2006; **281**: 28450–28459.
- Etienne-Manneville S, Hall A. Cell polarity: Par6, aPKC and cytoskeletal crosstalk. *Curr Opin Cell Biol* 2003; **15**: 67–72.
- Eder AM, Sui X, Rosen DG, Nolden LK, Cheng KW, Lahad JP et al. Atypical PKC*delta* contributes to poor prognosis through loss of apical-basal polarity and cyclin E overexpression in ovarian cancer. *Proc Natl Acad Sci USA* 2005; **102**: 12519–12524.
- Regala RP, Weems C, Jamieson L, Copland JA, Thompson EA, Fields AP. Atypical protein kinase Ciota plays a critical role in human lung cancer cell growth and tumorigenicity. *J Biol Chem* 2005; **280**: 31109–31115.
- Stallings-Mann M, Jamieson L, Regala RP, Weems C, Murray NR, Fields AP. A novel small-molecule inhibitor of protein kinase Ciota blocks transformed growth of non-small-cell lung cancer cells. *Cancer Res* 2006; **66**: 1767–1774.
- Gunaratne A, Thai BL, Di Guglielmo GM. Atypical protein kinase C phosphorylates Par6 and facilitates transforming growth factor beta-induced epithelial-to-mesenchymal transition. *Mol Cell Biol* 2013; **33**: 874–886.
- Bratt J, Belcher J, Vercellotti GM, Palmblad J. Effects of anti-rheumatic gold salts on NF-kappa B mobilization and tumour necrosis factor-alpha (TNF-alpha)-induced neutrophil-dependent cytotoxicity for human endothelial cells. *Clin Exp Immunol* 2000; **120**: 79–84.
- Yamashita M, Ashino S, Oshima Y, Kawamura S, Ohuchi K, Takayanagi M. Inhibition of TPA-induced NF-kappaB nuclear translocation and production of NO and PGE2 by the anti-rheumatic gold compounds. *J Pharm Pharmacol* 2003; **55**: 245–251.
- Jeon KI, Jeong JY, Jue DM. Thiol-reactive metal compounds inhibit NF-kappa B activation by blocking I kappa B kinase. *J Immunol* 2000; **164**: 5981–5989.
- Frederick LA, Matthews JA, Jamieson L, Justilien V, Thompson EA, Radisky DC et al. Matrix metalloproteinase-10 is a critical effector of protein kinase Ciota-Par6alpha-mediated lung cancer. *Oncogene* 2008; **27**: 4841–4853.
- Murray NR, Jamieson L, Yu W, Zhang J, Gokmen-Polar Y, Sier D et al. Protein kinase Ciota is required for Ras transformation and colon carcinogenesis *in vivo*. *J Cell Biol* 2004; **164**: 797–802.
- Lu Y, Jamieson L, Brasier AR, Fields AP. NF-kappaB/RelA transactivation is required for atypical protein kinase C iota-mediated cell survival. *Oncogene* 2001; **20**: 4777–4792.



Cell Death and Disease is an open-access journal published by Nature Publishing Group. This work is licensed under the Creative Commons Attribution-NonCommercial-No Derivative Works 3.0 Unported License. To view a copy of this license, visit <http://creativecommons.org/licenses/by-nc-nd/3.0/>

Supplementary Information accompanies this paper on Cell Death and Disease website (<http://www.nature.com/cddis>)